



Cite this: *Mater. Horiz.*, 2024, 11, 6504

Received 1st August 2024.
Accepted 10th October 2024

DOI: 10.1039/d4mh01010h

rsc.li/materials-horizons

Surface protection is essential when using wood as a construction material. However, the industry lacks sustainable alternatives to replace the presently dominant fossil-based synthetic water-resistant coatings. Here, we show a fully bio-based wood surface protection system using components sourced from birch bark and spruce bark, inspired by the natural barrier function of bark in trees. The coating formulation contains suberic acids and spruce bark polyphenols, resulting in a waterborne suspension that is safe and easy to apply to wood. The polyphenols play a dual role in the formulation as they stabilize the water-insoluble suberic acids and serve as nanofillers in the thermally cured coating, enabling the adjustment of the mechanical properties of the resulting coating. When applied to spruce wood, the coating formulation with 10% polyphenol and 90% suberic acids achieved a water absorption value of 100 g m^{-2} after 72 hours of water exposure, demonstrating superior performance compared to an alkyd emulsion coating. We conclude that instead of combusting tree bark, it can serve as a valuable resource for wood protection, closing the circle in the wood processing industry.

Introduction

Wood is one of the earliest construction materials employed in human history, exhibiting remarkable strength relative to its weight. The use of wood in outdoor construction applications has been increasing due to the advances in engineered wood products such as laminates and composites, as well as their advantages in terms of sustainability, renewability, and energy efficiency.¹ Despite this, there is still a significant demand for traditional wood cladding and sawn lumber products. However, these wood products face durability challenges when exposed to

Fully bio-based water-resistant wood coatings derived from tree bark[†]

Fengyang Wang, ^a Mohammad Morsali, ^{ab} Jānis Rīžikovs, ^c Ievgen Pylypchuk, ^a Aji P. Mathew ^a and Mika H. Sipponen ^{ab}

New concepts

We have demonstrated a new concept in wood surface protection by creating a fully bio-based system using components from birch bark and spruce bark, inspired by the natural barrier function of bark in trees. The uniqueness compared to existing research lies in our formulation, which is entirely derived from renewable resources, contrasting with the industry's reliance on fossil-based synthetic coatings. The use of spruce bark polyphenols not only stabilizes the water-insoluble suberic acids in a waterborne suspension but also serves as nanofillers, allowing for mechanical property adjustments in the coating—an innovative dual functionality. Our work provides new insight and underlying concept to the materials science by showcasing tree bark as a valuable resource for wood protection, achieving superior water resistance compared to traditional alkyd emulsion coatings. This research advances sustainable materials science and offers a practical solution for transforming waste into high-value products, thereby promoting resource-efficient use of forest resources.

moisture, heat, sunlight, and microorganisms.² To address this, applying a protective coating can insulate wood materials from the harsh outdoor environment, thereby prolonging their lifespan.

Traditional paints, varnishes, and drying oils are applied to wood as solutions or suspensions. However, wood coating formulations are often dissolved or dispersed in organic solvents, some of which contain hazardous compounds like ethylbenzene, benzene, formaldehyde, and heavy metals, which have a negative impact on human health and the surrounding environment.³ Moreover, these products contain synthetic polymers derived from fossil hydrocarbon resources.^{4,5} Therefore, sustainable, waterborne and fully biobased wood coatings are needed to minimize the environmental impact of the wood construction materials.⁶ It is important to note that waterborne coatings and coatings derived from bio-based materials have attracted considerable interest in recent years.⁷⁻⁹ However, a major challenge persists: most of these emerging coating systems still heavily rely on synthetic crosslinkers.^{10,11} In this study, we aim to develop a fully bio-based coating system from the compounds available from tree bark.

Tree bark is abundantly available from industrial wood processing locally, with the European Union alone producing

^a Department of Materials and Environmental Chemistry, Stockholm University, SE-10691, Stockholm, Sweden. E-mail: mika.sipponen@mmk.su.se

^b Department of Materials and Environmental Chemistry, Wallenberg Wood Science Center, Stockholm University, SE-10691, Stockholm, Sweden

^c Latvian State Institute of Wood Chemistry, Biorefinery Laboratory, Latvia

[†] Electronic supplementary information (ESI) available. See DOI: <https://doi.org/10.1039/d4mh01010h>



23 million metric tons per year.¹² Inspired by the natural barrier properties of bark,^{13,14} we started exploring it as a resource for wood protection in outdoor environments. Such an application holds immense potential to revolutionize the forest industry, shifting away from the current practice of burning tree bark for energy recovery towards utilizing it in carbon storing materials.¹⁵ A rich array of natural substances can be isolated from bark *via* alkaline and solvent extraction.^{16,17} These compounds, including hydrophobic molecules such as suberic acids and betulin, along with amphiphilic polyphenols, jointly form the protective tissue of bark.

Polyphenols and suberic acids obtained from spruce bark and birch outer bark¹⁸ are particularly interesting compounds owing to their surface activity and ability to undergo crosslinking.⁹ During birch bark fractionation, betulin is extracted *via* solvent extraction,¹⁵ and then the remaining suberin is hydrolyzed into suberic acids which include long-chain diacids, hydroxy acids, and short-chain aliphatic and aromatic acids.¹⁷ The obtained fatty acids are hydrophobic, and they are thermally curable at temperatures around 200 °C.¹⁹ Polyphenols can be extracted from spruce bark through a soda pulping technology.^{16,20} Polyphenols are natural crosslinkers used in materials such as hydrogels and polymer nanocomposites.^{21–23} Polyphenols can form covalent and non-covalent crosslinking structures when present in the thermoset formed from suberic acids *via* a polycondensation reaction.^{24,25}

Although bark extractives exhibit interesting properties in view of applications, the existing literature describes the use of bark-derived compounds as an additive in conventional wood coatings that still largely depend on fossil-based chemicals.^{26–29} Increased utilization of bark requires overcoming technical difficulties in achieving a water-resistant wood coating with bark-derived compounds. For example, suberic acids are highly viscous and water-insoluble, and their wax-like nature makes it difficult to coat them evenly without the use of organic solvents. Furthermore, bark-derived polyphenols, comprising a complex mixture of lignins and tannins, face a significant challenge due to their brittleness, hindering the formation of water-resistant films. It seems that the way forward, instead of using pure fractions of bark-derived compounds for coating formulations, is to mimic the composition of bark.

Here, we report a fully biobased and waterborne dispersion coating for wood protection by combining birch bark suberic acids and spruce bark polyphenols. Building on our previous work on stabilization of colloidal dispersions of fatty acids with softwood kraft lignin,³⁰ our approach to obtaining a stable waterborne coating involves stabilization of suberic acids in aqueous suspension by the amphiphilic polyphenols. The relatively more hydrophilic polyphenols form a polyelectrolyte surface on these so-called hybrid particles, allowing their homogeneous spreading on wood.²⁵ Upon thermal curing, the polyphenols become embedded in the polymeric network, tuning its mechanical, optical and chemical properties. The resulting fully biobased wood coating exhibits competitive water resistance and adhesion properties compared to the industrial benchmarks.

Results and discussion

The objective of this work was to develop a fully bio-based wood coating system based on compounds from tree bark alone. The suberic acids extracted from birch outer bark were identified as promising water barrier components because of their ability to undergo thermal curing, forming water-resistant, rubber-like thermosets. However, the stickiness and lack of solubility in water hinder the straightforward use of suberic acids for large-scale wood coating applications. Our approach to overcome the aforementioned challenges consisted of preparing hybrid nanoparticles of suberic acids with more hydrophilic polyphenols through the solvent exchange method, where the suberic acids and polyphenol are dissolved in a single pot and then precipitated out by adding water into the solution mixture, forcing the solute to reduce the contact area with water, resulting in the formation colloidal particle dispersions.³¹ The obtained particle dispersion can be concentrated to the ideal consistency and then be applied to the wood surface as a coating after curing (Fig. 1). Our findings reveal that the cured coating effectively protects wood against moisture. To gain a deeper understanding, we carefully characterized the coatings, starting with the dispersions of hybrid particles composed of suberic acids and polyphenols.

Our hypothesis was that by combining relatively more hydrophobic suberic acids with amphiphilic spruce bark polyphenols we can achieve colloidally dispersed particles that are well-suited for wood coating. Such a particulate coating relies on film-forming ability of the particles, and it was therefore pivotal to understand their appearance and features from macroscopic to microscopic length scales. When the polyphenol content of the particles was varied from 10% to 50%, the hybrid NP dispersions became gradually darker in appearance and the particles larger in size (Fig. 2a). DLS measurements confirmed that the hydrodynamic particle diameter increased from 170 nm at 10% polyphenol content to approximately 210 nm at 50% polyphenol content (Fig. 2c). Since the polyphenols were recovered from the spent alkaline cooking liquor by acidification, the pH of the dispersion decreased with increasing polyphenol content, and the zeta potential correspondingly increased from -35 mV to -17 mV due to the protonation of the carboxylic groups on the particle surface (Fig. 2d). These charged surfaces lend an explanation to the observed relation of the polyphenol content and apparent particle size: with lower polyphenol content the particles have less ionization and thus lower swelling in water. Upon drying, the particles with a low surface-coverage of hydrophilic moieties at polyphenol contents $\leq 30\%$ deform into flat morphologies with a thickness of around 7.5–10 nm (Fig. 2a). While the particles with more than 30% polyphenols tend to form more rigid particles that has less tendency to dissociate upon drying at room temperature, restricting the mobility of suberic acids.

Based on the AFM images in Fig. 2a, we speculate that the hybrid particles exhibit a range of structures, from thin bilayers to vesicles with various morphologies, as illustrated in Fig. 2b. The morphology of these hybrid particles is primarily influenced



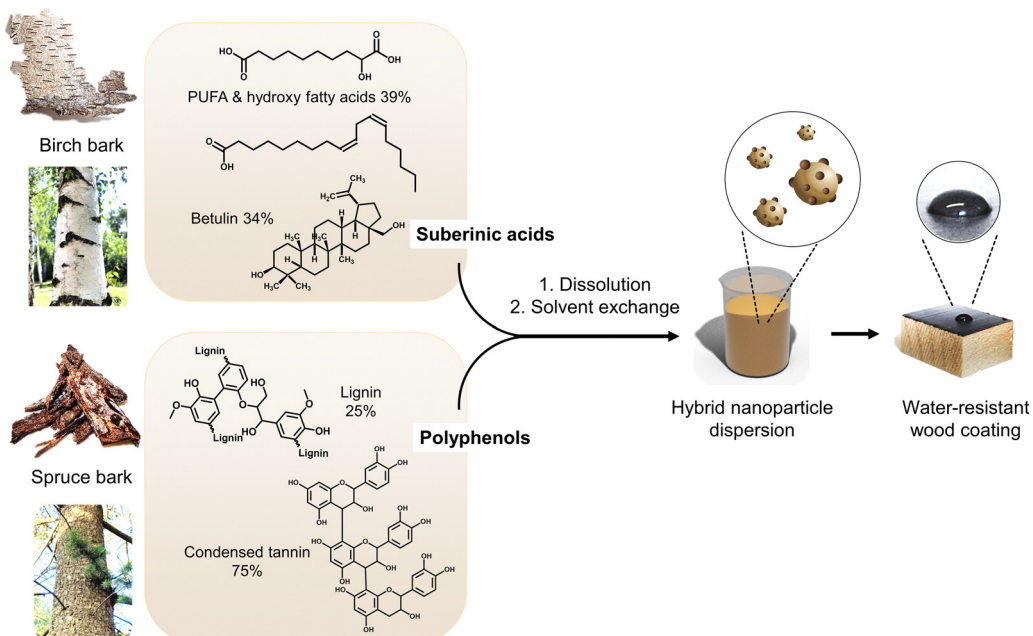


Fig. 1 Production of bark-derived water-resistant wood coating. Birch outer bark and spruce bark were used to extract suberic acids and polyphenols, which were then combined to form an aqueous dispersion coating. PUFA refers to polyunsaturated fatty acids.

by the volume ratio of the hydrophobic suberic acids to the hydrophilic polyphenols. The presence of polyphenols promotes the formation of closed vesicles with suberic acids, resulting in a relatively stable aqueous particle dispersion that minimizes aggregation and sedimentation. This stabilization effect contrasts with the behavior observed in pure suberic acid particles, as shown in the digital photograph and TEM image (Fig. S1, ESI[†]). To further investigate the native morphology of the vesicles, cryo-TEM images (Fig. 2e) of hybrid nanoparticles containing 30% polyphenol content were obtained, showing the vesicles in a hydrated state, appearing as spheres. Upon drying at room temperature, the vesicles collapsed and deformed, as revealed by the three-dimensional AFM images (Fig. 2f) and dry-state TEM images (Fig. S2, ESI[†]). Consistent with these findings, dehydration-induced deformation of bilayer vesicles has also been observed in amphiphilic block copolymers.³² Additionally, cryo-TEM images revealed the presence of complex particle geometries, including starfish-shaped vesicles, which have been previously reported.³³

Moreover, the interactions between the hybrid particles upon drying have significant practical implications for film formation, which is critical in developing water-resistant coatings. The spontaneous formation of a nanocomposite network upon drying of the dispersion coating is schematically shown in Fig. 3a and associated SEM and AFM images (Fig. 3b and c). The deformed particles form a network of polyphenol particles connected to each other *via* the waxy phase of suberic acids. Upon drying, the hybrid particles tend to aggregate, as the electric double-layer forces that usually separate them are no longer present, which previously was also observed in lignin oleate particles³⁴. Interestingly, the aggregated dried particles deform and lead to a series of connected hexagon-like networks

(Fig. 3b and c). This phenomenon is likely associated with interparticle interactions and surface energy dynamics that occur during the drying process of hybrid nanoparticles.³⁵ The presence of viscous suberic acids on the particle surface hinders particle rearrangement afterwards, which further results in the formation of three-dimensionally linked network through the fusing of suberic acids.²⁸ The flowing of suberic acids at the curing temperature, which is well above their melting point, allows their diffusion around polyphenols and the mass flow from convex to concave,³⁶ which decreases the porosity by filling the voids between particles, resulting in a coating with a relative smooth surface (see Fig. S3, ESI[†]).³⁷

To further investigate what happened to the hybrid particles during curing, the IR spectra of hybrid NP before and after curing were recorded (Fig. 4d). The IR spectra show that the absorption band at 1730 cm^{-1} significantly increased after curing, which indicates the formation of ester bonds in this process. At the same time, the band at 1625 cm^{-1} attributed to the stretching of carbonyl groups from free fatty acids and $\text{C}=\text{C}$ bond stretch in alkenes disappeared after curing, but reappeared after hydrolyzing the cured suberic acids (see Fig. S4, ESI[†]). Meanwhile, there is a significant decrease in intensity of the broad band at $3077\text{--}3650\text{ cm}^{-1}$ assigned to hydroxyl groups, which further indicates that the curing initiated a polycondensation reaction involving hydroxyl groups and carboxylic groups of the fatty acids. Similar observations were previously reported by Rizikovs and co-workers.³⁷ There is no clear difference among the IR spectra of cured hybrid NPs with different polyphenol content except the slight increase of intensity at 1166 cm^{-1} with increasing polyphenol content, which can be ascribed to the $\text{C}-\text{O}$ bond in the aromatic ring of polyphenol (Fig. S5, ESI[†]). Here, the curing onset temperature was observed around $160\text{ }^\circ\text{C}$, with

Increasing polyphenol content in hybrid NPs (wt %)

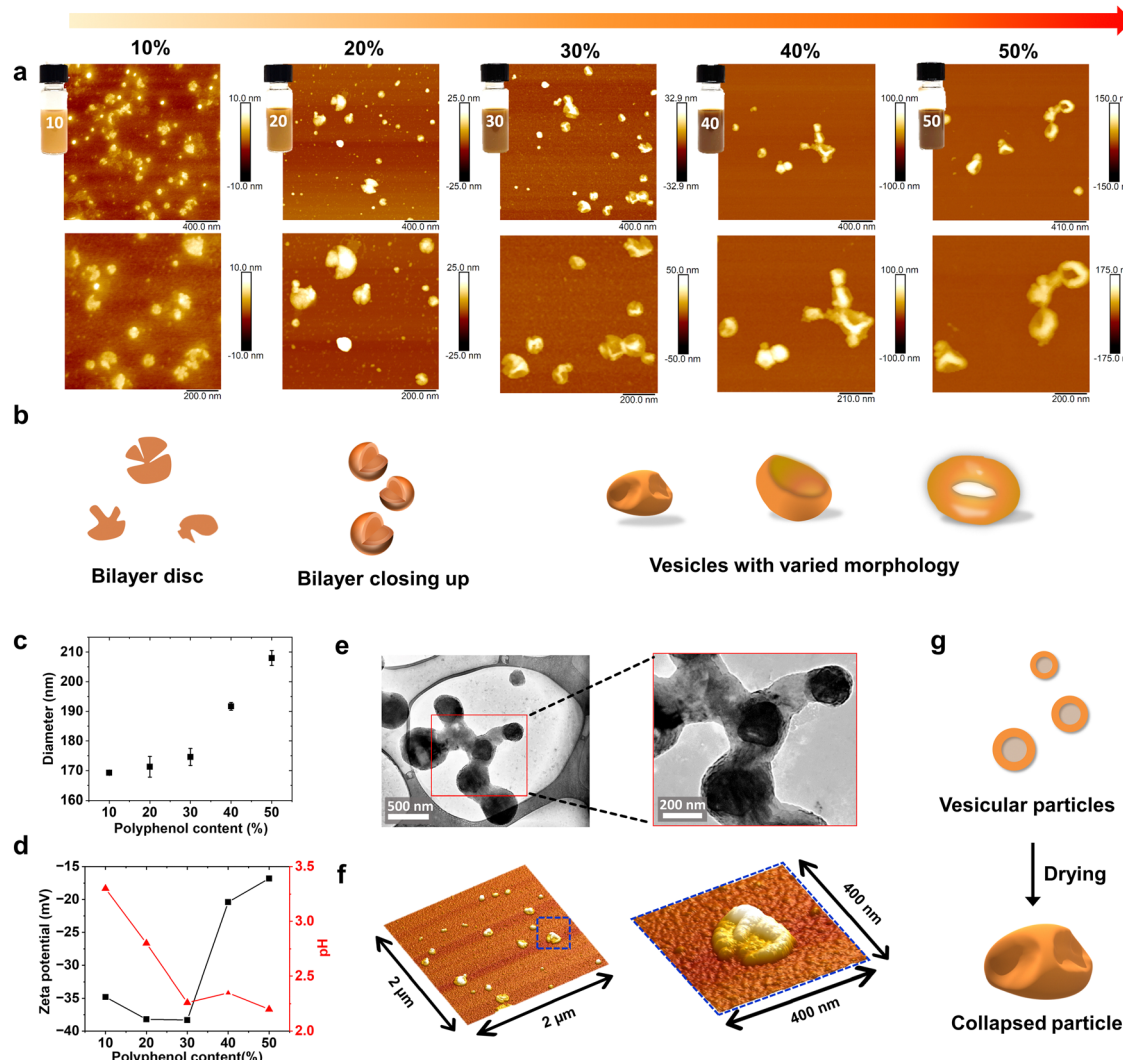


Fig. 2 Characterizations of the suberic acid-polyphenol nanoparticles. (a) AFM height images of the hybrid NPs at different magnifications and the digital images of the corresponding dispersion. (b) Illustration drawings indicate the morphology of the hybrid NPs. (c) The Z-average hydrodynamic particle diameter of hybrid NPs. (d) Zeta potential and pH of the hybrid NP dispersion. The morphology of the hybrid NPs with 30% polyphenol content: (e) Cryo-TEM images at different magnifications on a holey carbon film. (f) Effect of drying observed via three-dimensional AFM images at different magnifications. (g) Schematic illustration of the hybrid NPs morphology changes upon drying.

termination at approximately 220 °C regardless of the polyphenol content of the hybrid particles (Fig. 4a). Meanwhile, TGA traces recorded from pure suberic acids show onset of decomposition at around 329 °C, while the hybrid NP with 50% polyphenols started to decompose at a lower temperature of 298 °C (Fig. 4b). This difference can be ascribed to the varying thermal stability of polyphenols and suberic acids, the former starting to degrade at 268 °C but producing a high decomposition residue yield in an argon environment.

The reaction heat that was released from curing decreased significantly with more polyphenols, dropping 79% from 75 J g⁻¹ to 15.6 J g⁻¹ by increasing the polyphenol content from 10% to 50%. The black curve in Fig. 4c exhibits a linear relationship between the reaction heat and the polyphenol content. This behavior indicates that the phenolic hydroxyl

groups in spruce bark polyphenols are less reactive compared to the aliphatic hydroxyl groups present in suberic acids. Though the polyphenols reduced the enthalpy of the polycondensation reaction during the curing of the coating overall, it was found that a 10% polyphenol content in the hybrid particles resulted in 17% higher curing enthalpy compared to the case with pure suberic acids (Table 1). This energy balance means that the addition of 10% polyphenols to suberic acids promotes bond formation during the curing process. The contribution of suberic acids to the enthalpy can be derived by falsely assuming that the polyphenols are inert during the curing process. This exercise gives additional proof that that the polyphenols participated in the polycondensation reaction (Fig. 4c). The reactivity can also be influenced by the physical state of the reactants in terms of diffusion rate and intermolecular distance. For instance, the suberic acids melt

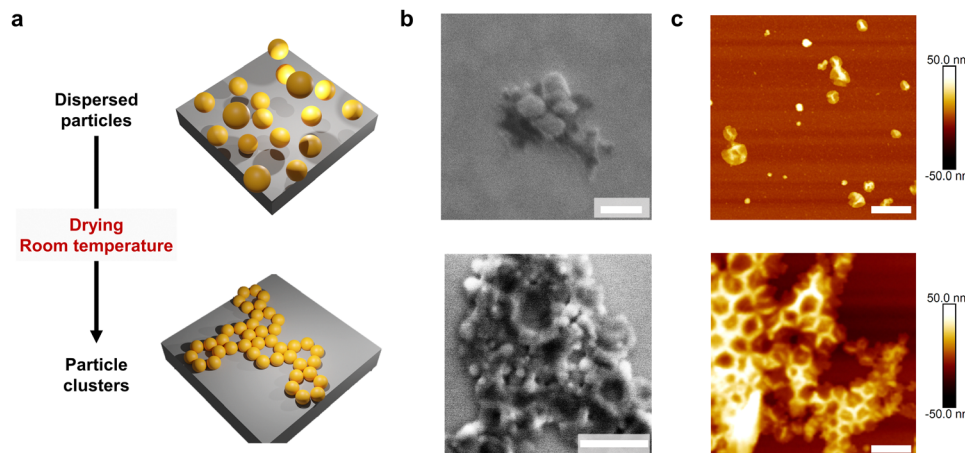


Fig. 3 The film formation process and drying-induced aggregation of the bark-derived particulate coating. (a) Schematic illustration of the film formation process of the hybrid NPs coating. (b) SEM images demonstrating the film formation process. (c) AFM images demonstrating the film formation process (hybrid particles with 30% polyphenol). Scale bar: 400 nm.

at around 50 °C, while spruce bark polyphenols remain solid during the reaction. The solid-state material has negligible intermolecular distance compared with liquids and gases, and the attraction force between the molecules is also much larger within solids.³⁸ While adding polyphenols beyond a 10% weight fraction results in an excess of covalently unreacted fraction in the formulation, the presence of polyphenols offers the ability to adjust the mechanical properties of the resulting nanocomposite coating.

Based on the thermal analysis above, the coating process with hybrid NPs includes casting, drying at room temperature under 40% relative humidity, and finally thermal curing for 45 minutes at 220 °C as illustrated in Fig. 5a. Mechanistically, the coalescence of suberic acids during curing provides strong crosslinking at the particle boundaries, which is favorable for achieving higher toughness in the coating. The polyphenols not only stabilize the particle dispersions but also help to evenly distribute the suberic acids, resulting in a uniform distribution

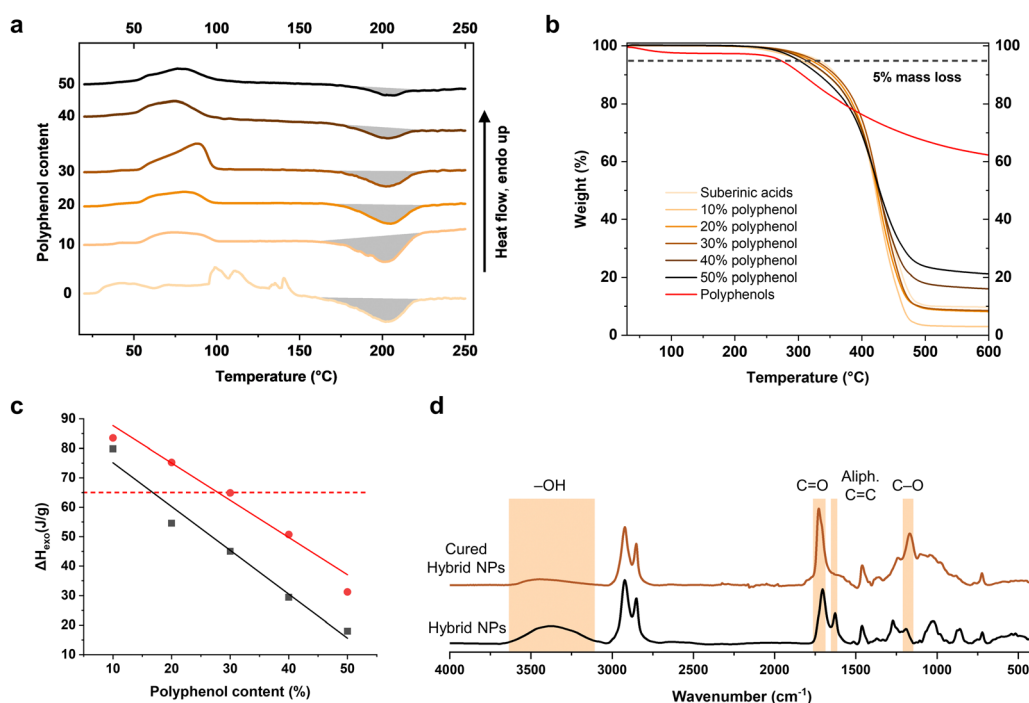


Fig. 4 The curing behavior of the bark-derived coatings. (a) The DSC curve of Hybrid NPs which shows the approximate curing temperature. (b) TGA curve of the cured hybrid NP coating with 30% polyphenol and pure suberic acids. (c) Enthalpy of different hybrid NPs curing reaction (black squares, linear fit with $R = -0.986$), and recalculated enthalpy based on the weight of suberic acids in the coating, polyphenol is considered inert (red circles, linear fit with $R = -0.988$). (d) FTIR spectrum of hybrid NP (30% polyphenol) before and after curing (background substrated).



Table 1 Characteristic temperature events from the DSC analysis of suberic acid-polyphenol particles with different polyphenol contents

Characteristic events	Polyphenol content of hybrid particles (wt%)					
	0	10	20	30	40	50
Onset cure temperature (°C)	165	163	156	161	163	164
Maximum peak temperature (°C)	203	202	204	204	203	204
Curing end temperature (°C)	225	235	225	225	220	221
Heat of reaction, ΔH_r (J g ⁻¹)	65	75	60	45	30.5	15.6

of crosslinked polyester and polyphenols at the nanoscale that resembles suberin naturally present in birch outer bark. In addition, the polyphenols act as a nanocomposite filler that provides tunable mechanical properties to the resulting polyester coatings that were tested for their water-resistance properties.

Water-resistance is essential for preserving wood products, especially those envisioned for outdoor use, as moisture can

cause dimensional changes in wood such as swelling and warping due to the abundance of hydrophilic hydroxyl groups in wood. The presence of water in wood products also creates an environment for fungi and other microbial degraders to thrive, which can lead to a decay process.³⁹ Therefore, we performed the water permeability test of the prepared coatings according to the EU standard EN927-5. The general setup of the water permeability test is illustrated in Fig. 5b. The test surface is brought to a face-down contact with water during the test, while all other surfaces of the wood block are sealed with an epoxy resin. The standard states that a stable construction is achieved when the water absorption value of the sample is below 175 g m⁻² after exposure to water for 72 hours.

Based on the measured water absorption values it was apparent that when the polyphenol content was 30% or below, the nanocomposite coatings fulfilled the standard requirements for stable construction (Fig. 5c). These values are

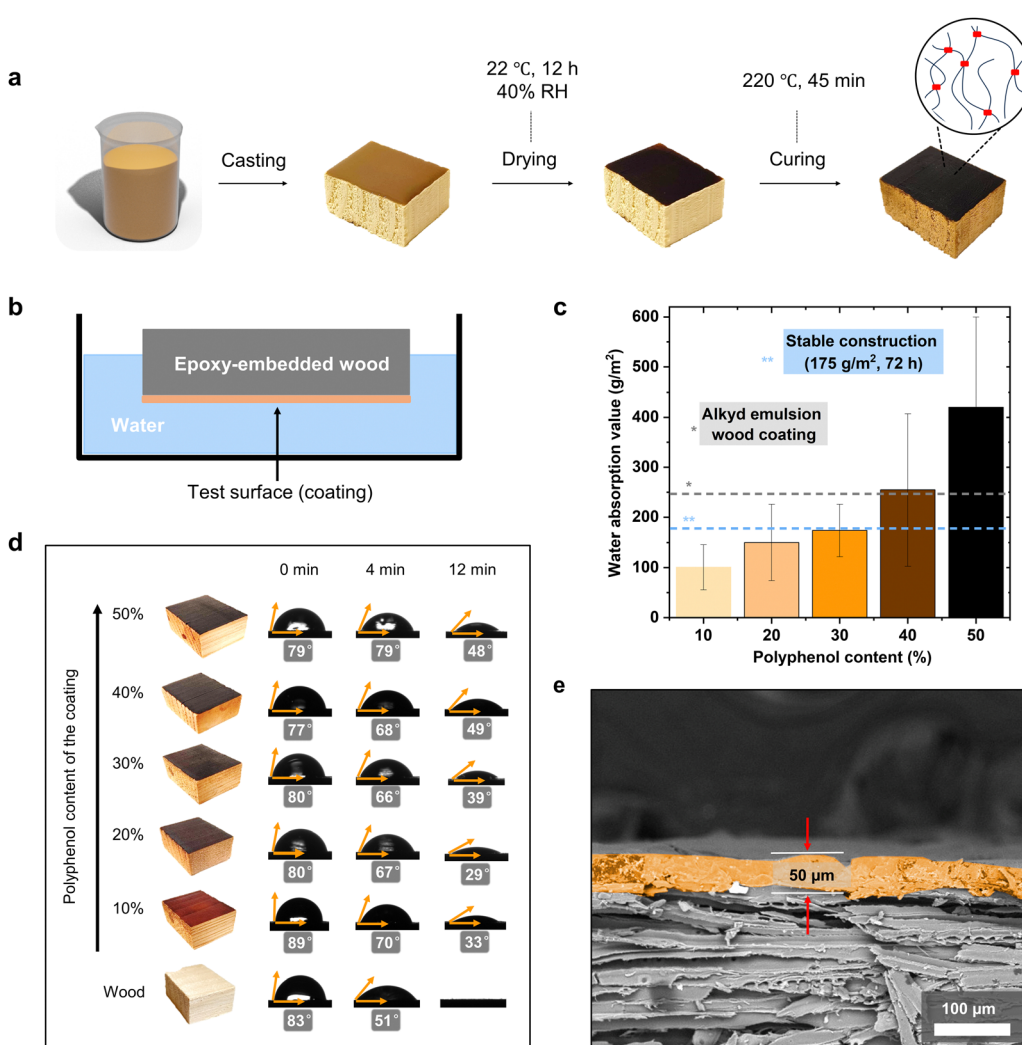


Fig. 5 Water-resistance of the bark-derived particulate coatings. (a) Schematic of the process of applying the prepared coating. (b) Illustration of the water permeability test. (c) Water absorption value of hybrid coatings with different polyphenol contents. (d) Digital photographs and water contact angles of non-coated wood and wood with nanocomposite coatings with different polyphenol contents. (e) SEM image of the cross-section of wood coated with a nanocomposite coating with 50 wt% polyphenol. The coating layer has been digitally colored orange for clarity.

comparable to the commercial alkyd emulsion wood coating.⁴⁰ However, it is important to note that the water absorption value increased greatly as the polyphenol content of the coating increased to 50%, which was due to an increased tendency of crack formation (Fig. S6, ESI†) despite the coating thickness of approximately 50 μm (Fig. 5e). In addition, the polyphenols increased the concentration of phenolic hydroxyl groups in the resulting coating, which tend to bind water. The visual appearance of the coating also changes with different polyphenol content, with a higher content of polyphenols leading to darker coating (Fig. 5d).

We further investigated how the coatings behave when they encounter water by measuring the water contact angle of each sample (see also Videos S1 and S2, ESI†). As shown in Fig. 5d above, all the wood mini-blocks that were coated with the prepared hybrid coatings show similar water contact angles of around 80° to 90°, which is typical for commercial polyesters like polyethylene terephthalate (PET) and polyester resin.^{41,42} With non-coated wood, the water contact angle dropped to 51° in 4 minutes, and all the water was absorbed in 12 minutes, while the coated wood samples became wetted slowly but did not absorb water within the same time period. Although the water contact angle values were at the borderline of hydrophobicity, the bark-derived coating protects wood from water just as effectively as the commercial alkyd emulsion wood coating. Considering the current surface structure of the coating, there remains potential to further enhance its hydrophobicity.

This could be achieved by optimizing factors such as surface roughness and the surface functional groups.^{43,44}

Given that this wood coating is intended for outdoor applications, it is crucial to assess its stain-resistant capabilities and adhesion to the wood surface. As depicted in Fig. 6a, the coated surface exhibits excellent stain resistance, leaving minimal traces after muddy water was applied on it, which is comparable to commercial alkyd emulsion coating as shown in Fig. S7 (ESI†). Additionally, it exhibits reduced wetting compared to the non-coated wood, which is also observed with the water contact angle measurements. Upon wiping away the residue of muddy water from the tested surface, the non-coated wood displays a brownish stain, whereas the coated wood appears clean and glossy.

Adherence to the wood surface is another critical parameter for a coating system. Fig. 6b below shows the result of the cross-cut test, which is a standard method to evaluate the resistance of a coating to separate from the substrate. The coatings with a polyphenol content below 30 wt% showed good adhesion towards the wood substrate as the images below demonstrated, which were classified as grade 4B out of 5B–0B, where grade 5B means that none of the cut squares is detached during the test, and grade 0B corresponds to detachment of over 65% of the squares. Therefore, the coating with 30 wt% polyphenol content is comparable to the commercial water-based acrylic painting (5B).²⁶ Samples with 40 and 50 wt% polyphenols were graded as 3B and 1B. As previously mentioned, the excessive

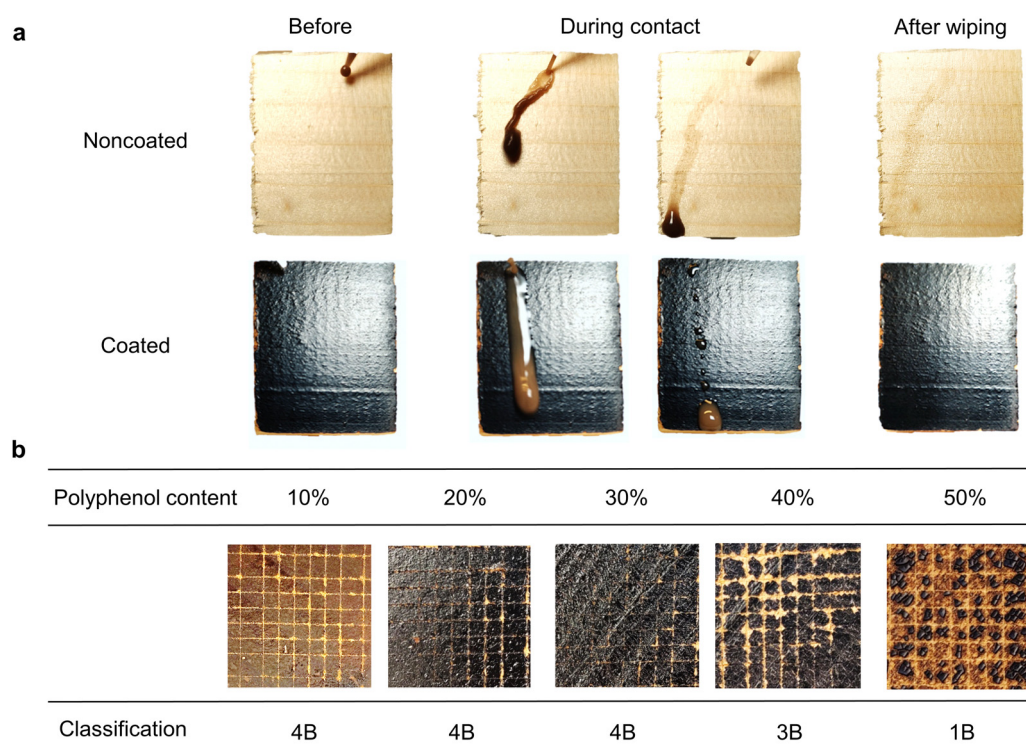


Fig. 6 Stain-resistance and classification of adhesion of the coating applied on spruce wood. (a) Digital photograph of uncoated and coated (hybrid NPs with 40% polyphenols) spruce wood before and after contact with muddy water. (b) Cross-cut test, resistance of paint coatings to separation from substrates according to ASTM D3359.



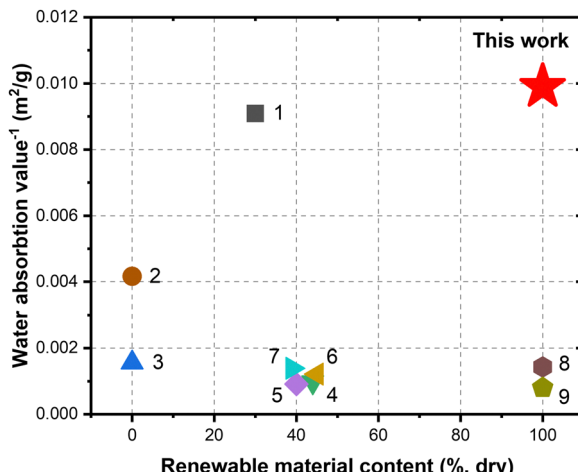


Fig. 7 Comparison of inverse of water absorption value to the biobased content of benchmark wood coating systems.^{40,50–54} The numbers in the graph refer to the list of references in Table S1 (ESI†).

concentration of polyphenols can hinder the bond formation between suberic acids, while the polyphenols on the other hand work as fillers, rendering the resulting coating more rigid but also brittle. This change in mechanical strength is indirectly reflected in the cross-cut result.

From a sustainability perspective, the fully bio-based wood coating presented in the current work stands out for its sole use of tree bark, a significant industrial waste from wood processing. By incorporating this otherwise underutilized material into the coating formulation, we not only reduce waste but also add value to a resource that is currently mainly combusted for energy generation.⁴⁵ This approach aligns with the principles of circular economy and resource efficiency, where materials are reused, recycled, or repurposed to minimize their environmental impacts.⁴⁶ Besides, many conventional coatings rely on harmful organic solvents and carcinogenic substances like formaldehyde or isocyanates.^{47–49} In terms of performance, when compared based on biobased content and water absorption value, the coating presented in the current work stands out from the state of the art (Fig. 7). The water absorption value of the fully bark-based coating was better across the field, even when compared to the systems low biobased contents between 25% and 40%. Overall, in addition to superior performance, our fully bark-derived coating formulation avoids the use of toxic compounds, making the coating more environmentally friendly and safer for the living environment.

Conclusions

We have reported the preparation of a fully bio-based wood coating which is entirely made from the main substances extracted from birch bark and spruce bark. The obtained water-borne coating can be thermally cured, leading to exceptional water resistance. In this coating formulation, the relatively hydrophilic polyphenols from spruce bark help disperse the hydrophobic wax-like birch bark extracted suberic acids in water, while altering the content of polyphenols can be used to

tune mechanical properties of the coating. Overall, we have shown that water-stable wood coating can be synthesized from tree bark extractives without chemical modification or using extraneous chemical additives, while the coating outperforms all known biobased systems and compares favorably with commercial products. We foresee these results will open up new opportunities in tree bark valorization with potential for exploration of applications beyond wood protection.

Experimental section

Materials

Suberic acids paste (FeCl_3 treated and dried) was received from the Latvian State Institute of Wood Chemistry,⁵⁵ Soda process black liquor (extracted from spruce bark through soda cooking process) was received from VTT Technical Research Centre of Finland Ltd, ethanol (D-sprit 95%) was purchased from Kilti Clean AB, sulfuric acid 95–97% was purchased from Sigma Aldrich, epoxy putty (Epoxispakel international water-tite 250 mL) was purchased from Bauhaus in Stockholm. Commercial alkyd wood coating used for stain resistance test was purchased from IKEA in Stockholm. Deionized water was used throughout the experiment.

Preparation of suberic acids/polyphenol hybrid nanoparticles

The spruce bark polyphenols were received from VTT as an alkaline (sodium hydroxide) spent cooking liquor that was acidified with sulfuric acid, and centrifuged to separate the precipitated polyphenols (10 000 rpm, 30 min). The obtained wet paste has a dry matter of 24.2 wt%, which was directly used in the later experiments. To prepare the hybrid NPs, 2.0 g of suberic acids was dissolved in ethanol/water binary solvent (50 g ethanol: 10 g water) together with different amounts of polyphenols (10%, 20%, 30%, 40%, 50% relative to the total dry mass) for at least 4 hours, then the insoluble part was removed by centrifugation and decanting (10 000 rpm, 15 min). The solution was then rapidly poured into 210 mL of water under vigorous stirring (800 rpm), the stirring continued for 30 minutes, and then the solvent was removed by evaporation. Hybrid NPs dispersions with around 1 wt% consistency were obtained at the end. Suberic acids particles in water were prepared in the same manner but without polyphenols in the formulation.

Preparation of wood protective coatings

The obtained hybrid NPs dispersions were centrifuged (10 000 rpm, 30 min) and re-dispersed into water to adjust the concentration to around 10 wt% for later use. 1 mL of the obtained dispersion was then applied on the tangential surface of a mini wood block (spruce, $37 \times 30 \times 12 \text{ mm}^3$). The applied dispersion was dried in a humidity chamber (23°C , 50% RH), and subsequently cured at 220°C for 45 minutes.

Liquid water permeability test

The coated mini wood blocks were used for the liquid water permeability test. According to EN927-5,⁵⁶ the uncoated faces



were sealed with moisture-impermeable coating. The sealed samples were conditioned overnight at 23 °C and 50% RH. After conditioning, samples were exposed to water by floating them in water with the coated surface facing down to the water. The exposure time was 72 h. The weight of samples was measured before and after the exposure to calculate the water absorption value.

Cross-cut adhesion test

The resistance of paint coatings to separate from substrates was tested according to ASTM D3359.⁵⁷ The multi-blade tool ZCC 2087 was used in this test. Two cuts were made with a 45° angle to the fibre direction, the second cut goes across the first one at 90°. Then the mini block was lightly brushed to remove loose particles. A 75 mm long tape piece was put in parallel to one of the cuts over the crosshatch pattern, smoothed and firmly rubbed with finger/fingernail. In the end, the tape steadily removed for 0.5 to 1.0 s at an angle which was close to 60° to the substrate. The result was evaluated based on how much of the coating was removed after the test.

Stain resistance test

The coating sample with 40% polyphenols was used for stain resistance test. The coated mini wood block was placed at a 60° angle on the table. 50 µL of muddy water was dropped onto the tested surface, and pictures were taken before, during, and after the contact with muddy water, as well as after cleaning the tested surface by pressing with a piece of paper towel. Muddy water was collected in front of Arrhenius Laboratory at Stockholm University and was not analyzed for composition.

Characterizations

FTIR-ATR. Varian 610-IR FT-IR spectrometer was used to acquire the (IR) absorbance of samples, it was measured in attenuated total reflection – Fourier transform infrared spectroscopic (ATR-FTIR) mode in the range of 450–4000 cm⁻¹.

Differential scanning calorimetry (DSC). Netzsch DSC 214 Polyma was used to acquire DSC data with N2 as the purge gas (50 mL min⁻¹) and a heating rate of 10 °C min⁻¹ in the 25–250 °C temperature range. Calibration was performed using an indium standard for heat flow calibration and zinc standard for temperature calibration.

Thermogravimetric analysis (TGA). TGA was performed using a TA Instruments Discovery TG with a platinum high-temperature pan. The temperature ramp was from 30 °C to 600 °C with a heating rate of 20 °C minute⁻¹ in argon environment.

Atomic force microscopy (AFM). Multimode-8 AFM (Bruker, USA) was operated at PeakForce Tapping mode with ScanAsyst algorithm self-optimization was used to acquire AFM images. ScanAsyst-air probes were used in all measurement. All the images were processed with Nanoscope Analysis 2.0 software.

Cryo-transmission electron microscopy (Cryo-TEM). JEM-2100F (JEOL Ltd, Japan) was used to acquire cryo-TEM images, an aliquot of the dispersion was diluted in deionized water, deposited over a TEM grid and frozen in liquid ethane.

The images were obtained under cooling with liquid nitrogen at an accelerating voltage of 200 kV.

Transmission electron microscopy (TEM). JEM-2100 microscope (JEOL Ltd, Japan) was used to acquire TEM image at an accelerating voltage of 200 kV. Colloidal water dispersion of hybrid NPs were diluted by a factor of 1:100, followed by the deposition onto a carbon coated copper grid and evaporation of water.

Dynamic light scattering (DLS). Hydrodynamic particle size was measured with a Zetasizer Nano ZS (Malvern, UK). The zeta potential was determined using a dip cell probe. Samples were appropriately diluted prior to the test.

Water contact angle. Water contact angle was measured with KRÜSS instruments Drop Shape Analyzer – DSA25, 2 µL water drop was used. All the images were processed with the ADVANCE software.

Scanning electron microscopy (SEM). SEM images of hybrid NPs were taken with JEOL JSM-7000F (JEOL Ltd, Japan) operating at 2–5 kV, particle dispersion was diluted before the experiment, followed by depositing 10 µL of diluted dispersion on a UV/ozone treated silicon wafer. The images of the cross-section of coated wood were taken with Hitachi TM3000.

Author contributions

Fengyang Wang: conceptualization, methodology, investigation. Writing – original draft, writing – reviewing & editing, visualization, project administration. Mohammad Morsali: methodology, investigation, writing – reviewing & editing, visualization. Jānis Rižikovs: resources, writing – reviewing & editing, Ievgen Pylypchuk: methodology, investigation, writing – reviewing & editing, visualization, project administration. Aji P. Mathew: conceptualization, writing – reviewing & editing. Milka Sipponen: conceptualization, methodology, validation, writing – reviewing & editing, visualization, resources, supervision, project administration, funding acquisition.

Data availability

The source data supporting the findings of this study are available at <https://doi.org/10.5281/zenodo.13148372>.

Conflicts of interest

There are no conflicts to declare.

Acknowledgements

The authors acknowledge funding from Energimyndigheten, Formas and Vinnova (Grant Number 2021-05015) within the project BarkBuild supported under the umbrella of ERA-NET Cofund Action ForestValue (773324). M. H. S. acknowledges funding from the Knut and Alice Wallenberg Foundation (KAW) through the Wallenberg Wood Science Center (grant number KAW 2021.0313). Dr Marc Borrega (VTT, Finland) is



acknowledged for supplying the spruce bark polyphenols and constructive discussions.

References

- Y. Ding, Z. Pang, K. Lan, Y. Yao, G. Panzarasa, L. Xu, M. Lo Ricco, D. R. Rammer, J. Y. Zhu, M. Hu, X. Pan, T. Li, I. Burgert and L. Hu, Emerging Engineered Wood for Building Applications, *Chem. Rev.*, 2023, **123**(5), 1843–1888, DOI: [10.1021/acs.chemrev.2c00450](https://doi.org/10.1021/acs.chemrev.2c00450).
- M. De Meijer, Review on the Durability of Exterior Wood Coatings with Reduced VOC-Content, *Prog. Org. Coat.*, 2001, **43**, 217–225.
- T. V. Dinh, I. Y. Choi, Y. S. Son, K. Y. Song, Y. Sunwoo and J. C. Kim, Volatile Organic Compounds (VOCs) in Surface Coating Materials: Their Compositions and Potential as an Alternative Fuel, *J. Environ. Manage.*, 2016, **168**, 157–164, DOI: [10.1016/j.jenvman.2015.11.059](https://doi.org/10.1016/j.jenvman.2015.11.059).
- F. Bulian and J. Graystone, *Wood Coatings: Theory and Practice*, 2009, p. 320.
- R. Lambourne and T. A. Strivens, *Paint and Surface Coatings: Theory and Practice*, 1999, p. 784.
- C.-A. Teacă, D. Roșu, F. Mustață, T. Rusu, L. Roșu, I. Roșca and C.-D. Varganică, Natural Bio-Based Products for Wood Coating and Protection against Degradation: A Review, *BioResources*, 2019, **14**(2), 4877–4878.
- M. N. Khan, C. M. Clarkson, M. Nuruddin, A. Sharif, E. Ahmad and J. P. Youngblood, Performance of Advanced Waterborne Wood Coatings Reinforced with Cellulose Nanocrystals, *ACS Appl. Bio Mater.*, 2022, **5**(9), 4179–4190, DOI: [10.1021/acsabm.2c00383](https://doi.org/10.1021/acsabm.2c00383).
- J. Janesch, M. Bacher, S. Padhi, T. Rosenau, W. Gindl-Altmutter and C. Hansmann, Biobased Alkyd Resins from Plant Oil and Furan-2,5-Dicarboxylic Acid, *ACS Sustainable Chem. Eng.*, 2023, **11**(50), 17625–17632, DOI: [10.1021/acsuschemeng.3c04346](https://doi.org/10.1021/acsuschemeng.3c04346).
- X. Song, S. Tang, X. Chi, G. Han, L. Bai, S. Q. Shi, Z. Zhu and W. Cheng, Valorization of Lignin from Biorefinery: Colloidal Lignin Micro-Nanospheres as Multifunctional Bio-Based Fillers for Waterborne Wood Coating Enhancement, *ACS Sustainable Chem. Eng.*, 2022, **10**(35), 11655–11665, DOI: [10.1021/acsuschemeng.2c03590](https://doi.org/10.1021/acsuschemeng.2c03590).
- P. L. De Hoyos-Martínez, H. Issaoui, R. Herrera, J. Labidi and F. Charrier-El Bouhout, Wood Fireproofing Coatings Based on Biobased Phenolic Resins, *ACS Sustainable Chem. Eng.*, 2021, **9**(4), 1729–1740, DOI: [10.1021/acsuschemeng.0c07505](https://doi.org/10.1021/acsuschemeng.0c07505).
- L. De Viguerie, P. A. Payard, E. Portero, P. Walter and M. Cotte, The Drying of Linseed Oil Investigated by Fourier Transform Infrared Spectroscopy: Historical Recipes and Influence of Lead Compounds, *Prog. Org. Coat.*, 2016, **93**, 46–60, DOI: [10.1016/j.porgcoat.2015.12.010](https://doi.org/10.1016/j.porgcoat.2015.12.010).
- A. Thorenz, L. Wietschel, D. Stindt and A. Tuma, Assessment of Agroforestry Residue Potentials for the Bioeconomy in the European Union, *J. Cleaner Prod.*, 2018, **176**, 348–359, DOI: [10.1016/j.jclepro.2017.12.143](https://doi.org/10.1016/j.jclepro.2017.12.143).
- D. Li, R. Moriana and M. Ek, From Forest Residues to Hydrophobic Nanocomposites with High Oxygen-Barrier Properties, *Nord. Pulp Pap. Res. J.*, 2016, **31**(2), 261–269, DOI: [10.3183/npprj-2016-31-02-p261-269](https://doi.org/10.3183/npprj-2016-31-02-p261-269).
- X. Niu, E. J. Foster, B. O. Patrick, O. J. Rojas, X. Niu, E. J. Foster, O. J. Rojas and B. O. Patrick, Betulin Self-Assembly: From High Axial Aspect Crystals to Hedgehog Suprastructures, *Adv. Funct. Mater.*, 2022, **32**(44), 2206058, DOI: [10.1002/adfm.202206058](https://doi.org/10.1002/adfm.202206058).
- J. Rizhikovs, J. Zandersons, G. Dobeļe and A. Paze, Isolation of Triterpene-Rich Extracts from Outer Birch Bark by Hot Water and Alkaline Pre-Treatment or the Appropriate Choice of Solvents, *Ind. Crops Prod.*, 2015, **76**, 209–214, DOI: [10.1016/j.indcrop.2015.06.053](https://doi.org/10.1016/j.indcrop.2015.06.053).
- M. Borrega, A. Kalliola, M. Määttänen, A. S. Borisova, A. Mikkelsen and T. Tamminen, Alkaline Extraction of Polyphenols for Valorization of Industrial Spruce Bark, *Bioresour. Technol. Rep.*, 2022, **19**, 101129, DOI: [10.1016/j.biteb.2022.101129](https://doi.org/10.1016/j.biteb.2022.101129).
- J. Rizhikovs, P. Brazdauskas, A. Paze, R. Tupčiauskas, J. Grinins, M. Puke, A. Plavniček, M. Andzs, D. Godina and R. Makars, Characterization of Subericin Acids from Birch Outer Bark as Bio-Based Adhesive in Wood Composites, *Int. J. Adhes. Adhes.*, 2022, **112**, DOI: [10.1016/j.ijadhadh.2021.102989](https://doi.org/10.1016/j.ijadhadh.2021.102989).
- P. E. Kolattukudy, Biopolyester Membranes of Plants: Cutin and Suberin, *Science*, 1980, **208**(4447), 990–1000, DOI: [10.1126/science.208.4447.990](https://doi.org/10.1126/science.208.4447.990).
- R. Makars, J. Rizikovs and A. Paze, Study of Catalysts for Subericin Acid-Based Adhesive Polymerization, *Materials Science Forum*, Trans Tech Publications Ltd, 2022, vol. 1071, pp. 182–188, DOI: [10.4028/p-gxs1x9](https://doi.org/10.4028/p-gxs1x9).
- K. Kemppainen, M. Siika-aho, S. Pattathil, S. Giovando and K. Kruus, Spruce Bark as an Industrial Source of Condensed Tannins and Non-Cellulosic Sugars, *Ind. Crops Prod.*, 2014, **52**, 158–168, DOI: [10.1016/j.indcrop.2013.10.009](https://doi.org/10.1016/j.indcrop.2013.10.009).
- H. Fan, J. Wang and Z. Jin, Tough, Swelling-Resistant, Self-Healing, and Adhesive Dual-Cross-Linked Hydrogels Based on Polymer-Tannic Acid Multiple Hydrogen Bonds, *Macromolecules*, 2018, **51**(5), 1696–1705, DOI: [10.1021/acs.macromol.7b02653](https://doi.org/10.1021/acs.macromol.7b02653).
- H. Fan, L. Wang, X. Feng, Y. Bu, D. Wu and Z. Jin, Supramolecular Hydrogel Formation Based on Tannic Acid, *Macromolecules*, 2017, **50**(2), 666–676, DOI: [10.1021/acs.macromol.6b02106](https://doi.org/10.1021/acs.macromol.6b02106).
- V. Rubenthaler, T. A. Ward, C. Y. Chee and C. K. Tang, Processing and Analysis of Chitosan Nanocomposites Reinforced with Chitin Whiskers and Tannic Acid as a Cross-linker, *Carbohydr. Polym.*, 2015, **115**, 379–387, DOI: [10.1016/j.carbpol.2014.09.007](https://doi.org/10.1016/j.carbpol.2014.09.007).
- C. Chen; H. Yang; X. Yang and Q. Ma, Tannic Acid: A Crosslinker Leading to Versatile Functional Polymeric Networks: A Review, *RSC Advances*, Royal Society of Chemistry, 2022, pp. 7689–7711, DOI: [10.1039/d1ra07657d](https://doi.org/10.1039/d1ra07657d).
- S. Rivero, M. A. García and A. Pinotti, Crosslinking Capacity of Tannic Acid in Plasticized Chitosan Films, *Carbohydr. Polym.*, 2010, **82**(2), 270–276, DOI: [10.1016/j.carbpol.2010.04.048](https://doi.org/10.1016/j.carbpol.2010.04.048).
- Y. Huang, Q. Feng, C. Ye, S. S. Nair and N. Yan, Incorporation of Ligno-Cellulose Nanofibrils and Bark Extractives in



Water-Based Coatings for Improved Wood Protection, *Prog. Org. Coat.*, 2020, **138**, 105210, DOI: [10.1016/j.porgcoat.2019.105210](https://doi.org/10.1016/j.porgcoat.2019.105210).

27 A. Kumar, R. Korpinen, V. Möttönen and E. Verkasalo, Suberin Fatty Acid Hydrolysates from Outer Birch Bark for Hydrophobic Coating on Aspen Wood Surface, *Polymers*, 2022, **14**(4), 832, DOI: [10.3390/polym14040832](https://doi.org/10.3390/polym14040832).

28 S. Saha, D. Kocaefe, Y. Boluk and A. Pichette, Enhancing Exterior Durability of Jack Pine by Photo-Stabilization of Acrylic Polyurethane Coating Using Bark Extract. Part 1: Effect of UV on Color Change and ATR-FT-IR Analysis, *Prog. Org. Coat.*, 2011, **70**(4), 376–382, DOI: [10.1016/j.porgcoat.2010.09.034](https://doi.org/10.1016/j.porgcoat.2010.09.034).

29 E. M. Tudor, M. C. Barbu, A. Petutschnigg and R. Réh, Added-Value for Wood Bark as a Coating Layer for Flooring Tiles, *J. Cleaner Prod.*, 2018, **170**, 1354–1360, DOI: [10.1016/j.jclepro.2017.09.156](https://doi.org/10.1016/j.jclepro.2017.09.156).

30 M. H. Sipponen, A. Henn, P. Penttilä and M. Österberg, Lignin-Fatty Acid Hybrid Nanocapsules for Scalable Thermal Energy Storage in Phase-Change Materials, *Chem. Eng. J.*, 2020, **393**, 124711, DOI: [10.1016/j.cej.2020.124711](https://doi.org/10.1016/j.cej.2020.124711).

31 M. Österberg, M. H. Sipponen, B. D. Mattos and O. J. Rojas, Spherical Lignin Particles: A Review on Their Sustainability and Applications, *Green Chem.*, 2020, **22**(9), 2712–2733, DOI: [10.1039/d0gc00096e](https://doi.org/10.1039/d0gc00096e).

32 R. S. M. Rikken, H. Engelkamp, R. J. M. Nolte, J. C. Maan, J. C. M. Van Hest, D. A. Wilson and P. C. M. Christianen, Shaping Polymersomes into Predictable Morphologies via Out-of-Equilibrium Self-Assembly, *Nat. Commun.*, 2016, **7**(1), 1–7, DOI: [10.1038/ncomms12606](https://doi.org/10.1038/ncomms12606).

33 J. Sun, S. Kleuskens, J. Luan, D. Wang, S. Zhang, W. Li, G. Uysal and D. A. Wilson, Morphogenesis of Starfish Polymersomes, *Nat. Commun.*, 2023, **14**(1), 1–11, DOI: [10.1038/s41467-023-39305-8](https://doi.org/10.1038/s41467-023-39305-8).

34 A. Moreno, J. Liu, R. Gueret, S. E. Hadi, L. Bergström, A. Slabon and M. H. Sipponen, Unravelling the Hydration Barrier of Lignin Oleate Nanoparticles for Acid- and Base-Catalyzed Functionalization in Dispersion State, *Angew. Chem., Int. Ed.*, 2021, **60**(38), 20897–20905, DOI: [10.1002/anie.202106743](https://doi.org/10.1002/anie.202106743).

35 R. A. L. Jones, Soft Condensed Matter, *Oxford master series in condensed matter physics*, Oxford University Press, Oxford [England], 2002, vol. 6.

36 U. Schubert and N. Hüsing, *Synthesis of Inorganic Materials*, Wiley-VCH, 2019.

37 J. Rizikovs, D. Godina, R. Makars, A. Paze, A. Abolins, A. Fridrihsone, K. Meile and M. Kirpluks, Subericin Acids as a Potential Feedstock for Polyol Synthesis: Separation and Characterization, *Polymers*, 2021, **13**(24), 4380, DOI: [10.3390/polym13244380](https://doi.org/10.3390/polym13244380).

38 L. R. Macgillivray, G. S. Papaefstathiou, T. Friščić, T. D. Hamilton, D. K. Bučar, Q. Chu, D. B. Varshney and I. G. Georgiev, Supramolecular Control of Reactivity in the Solid State: From Templates to Ladderanes to Metal-Organic Frameworks, *Acc. Chem. Res.*, 2008, **41**(2), 280–291, DOI: [10.1021/ar700145r](https://doi.org/10.1021/ar700145r).

39 A. Cataldi, C. Esposito Corcione, M. Frigione and A. Pegoretti, Photocurable Resin/Nanocellulose Composite Coatings for Wood Protection, *Prog. Org. Coat.*, 2017, **106**, 128–136, DOI: [10.1016/j.porgcoat.2017.01.019](https://doi.org/10.1016/j.porgcoat.2017.01.019).

40 J. Ekstedt and G. Östberg, Liquid Water Permeability of Exterior Wood Coatings-Testing According to a Proposed European Standard Method, *J. Coat. Technol.*, 2001, **73**(914), 53–59, DOI: [10.1007/bf02698438/metrics](https://doi.org/10.1007/bf02698438/metrics).

41 Y. Fu, M. Soldera, W. Wang and S. Milles, Reports, K. D.-S.; 2020, undefined, Wettability Control of Polymeric Microstructures Replicated from Laser-Patterned Stamps, *nature.com*.

42 R. Ploeger, S. Musso and O. Chiantore, Contact Angle Measurements to Determine the Rate of Surface Oxidation of Artists' Alkyd Paints during Accelerated Photo-Ageing, *Prog. Org. Coat.*, 2009, **65**(1), 77–83, DOI: [10.1016/j.porgcoat.2008.09.018](https://doi.org/10.1016/j.porgcoat.2008.09.018).

43 X. Xu, Y. Zhang, J. Wen, Z. Zhang, T. Xin, D. Yu, X. Wu, Q. Yao, J. Fan and X. Peng, Large-Area, Daily, on-Site-Applicable Antiahesion Coatings Formed via Ambient Self-Crosslinking, *Chem. Eng. J.*, 2022, **450**, 138156, DOI: [10.1016/j.cej.2022.138156](https://doi.org/10.1016/j.cej.2022.138156).

44 X. Jiang, X. Xu, Z. Xia, D. Lin, Y. Chen, Y. Wang, D. Yu, X. Wu and H. Zeng, Simultaneous Segment Orientation and Anchoring for Robust Hydrogel Coating with Underwater Superoleophobility, *Adv. Funct. Mater.*, 2024, **34**(24), 2314589, DOI: [10.1002/adfm.202314589](https://doi.org/10.1002/adfm.202314589).

45 S. Feng, S. Cheng, Z. Yuan, M. Leitch and C. Xu, Valorization of Bark for Chemicals and Materials: A Review, *Renewable Sustainable Energy Rev.*, 2013, **26**, 560–578, DOI: [10.1016/j.rser.2013.06.024](https://doi.org/10.1016/j.rser.2013.06.024).

46 B. Kiser, Circular Economy: Getting the Circulation Going, *Nature*, 2016, **531**(7595), 443–446, DOI: [10.1038/531443a](https://doi.org/10.1038/531443a).

47 A. Gomez-Lopez, S. Panchireddy, B. Grignard, I. Calvo, C. Jerome, C. Detrembleur and H. Sardon, Poly(Hydroxyurethane) Adhesives and Coatings: State-of-the-Art and Future Directions, *ACS Sustainable Chem. Eng.*, 2021, **9**(29), 9541–9562, DOI: [10.1021/acssuschemeng.1c02558](https://doi.org/10.1021/acssuschemeng.1c02558).

48 Y. Liu, C. Zeng, M. Wang, X. Shao, Y. Yao, G. Wang, Y. Li, M. Hou, L. Fan and D. Ye, Characteristics and Environmental and Health Impacts of Volatile Organic Compounds in Furniture Manufacturing with Different Coating Types in the Pearl River Delta, *J. Cleaner Prod.*, 2023, **397**, 136599, DOI: [10.1016/j.jclepro.2023.136599](https://doi.org/10.1016/j.jclepro.2023.136599).

49 Chemicals: The EU restricts exposure to carcinogenic substance formaldehyde in consumer products - European Commission, https://single-market-economy.ec.europa.eu/news/chemicals-eu-restricts-exposure-carcinogenic-substance-formaldehyde-consumer-products-2023-07-14_en, accessed 2024-03-14.

50 M. Calovi, V. Coroneo and S. Rossi, Antibacterial Efficiency over Time and Barrier Properties of Wood Coatings with Colloidal Silver, *Appl. Microbiol. Biotechnol.*, 2023, **107**(19), 5975–5986, DOI: [10.1007/s00253-023-12710-1/figures/7](https://doi.org/10.1007/s00253-023-12710-1/figures/7).

51 M. Calovi and S. Rossi, The Impact of Stainless Steel Flakes as a Novel Multifunctional Pigment for Wood Coatings, *J. Coat. Technol. Res.*, 2024, **21**(3), 1031–1047, DOI: [10.1007/s11998-023-00870-8/figures/15](https://doi.org/10.1007/s11998-023-00870-8/figures/15).



52 M. Calovi and S. Rossi, From Wood Waste to Wood Protection: New Application of Black Bio Renewable Water-Based Dispersions as Pigment for Bio-Based Wood Paint, *Prog. Org. Coat.*, 2023, **180**, 107577, DOI: [10.1016/j.porgcoat.2023.107577](https://doi.org/10.1016/j.porgcoat.2023.107577).

53 D. Angelski and K. Atanasova, Water Permeability and Adhesion Strength of Bio-Based Coating Applied on Wood, *Drvna industrija*, 2024, **75**(1), 43–48, DOI: [10.5552/drwind.2024.0118](https://doi.org/10.5552/drwind.2024.0118).

54 M. Humar and B. Lesar, Efficacy of Linseed- and Tung-Oil-Treated Wood against Wood-Decay Fungi and Water Uptake, *Int. Biodeterior. Biodegrad.*, 2013, **85**, 223–227, DOI: [10.1016/j.ibiod.2013.07.011](https://doi.org/10.1016/j.ibiod.2013.07.011).

55 D. Godina, R. Makars, A. Paze and J. Rizhikovs, Analytical Method Cluster Development for Comprehensive Characterisation of Subericin Acids Derived from Birch Outer Bark, *Molecules*, 2023, **28**(5), 2227, DOI: [10.3390/molecules28052227](https://doi.org/10.3390/molecules28052227).

56 EN 927-5, Paint and Varnishes – Coating Materials and Coating Systems for Exterior Wood – Part 5: Assessment of the Liquid Water Permeability, European Committee for Standardization, Brussels 2000.

57 ASTM D3359-17, Standard Test Methods for Rating Adhesion by Tape Test, ASTM International, 2017.